

# **ATLANTIC-WIDE RESEARCH PROGRAMME ON BLUEFIN TUNA (GBYP - 2010)**

## **Data Recovery Plan – Elaboration of 2010 Data from the Aerial Survey on Spawning Aggregations**

### **Final Report**

**27 September 2010**

**Ana Cañadas, Philip Hammond & José Antonio Vázquez**

Alnilam Research and Conservation Ltd

Cádamo 116, La Berzosa, 28240 Hoyo de Manzanares, Madrid, Spain

### **Background**

The comprehensive ICCAT Atlantic Wide Research Programme on Bluefin Tuna (GBYP) aims to improve basic data collection, understanding of key biological and ecological processes, and assessment models and management. An important element of this programme is to carry out aerial line transect surveys of the spawning population in the Mediterranean when and where schools can traditionally be sighted close to the surface to support development of fishery-independent indices. This report describes the analysis for those aerial surveys.

### **Objectives**

To summarise the original design with any subsequent modifications

To summarise the first year's results including: maps of transects with sightings; analysis of data including estimation of detection probability with covariates; generation of preliminary estimates of density and abundance with CVs in each of the survey areas, including both indices and spatial temporal distributions.

To review the survey design including: its use in providing a fishery-independent index, e.g. absolute estimate *vs* index; a power analysis to investigate the effect of increasing precision.

To make recommendations related to: changes to the design in order to better meet scientific and management objectives; use in assessment and management.

To inform the design for a Future Survey Work Plan.

### **Data**

#### **Survey design**

The data for analysis were collected on aerial surveys designed by the proposers as a line transect sampling survey using software DISTANCE <http://www.ruwpa.st-and.ac.uk/distance/>, the “industry standard” software for line and point transect distance sampling (Hammond, Cañadas & Vázquez 2010).

Surveys were designed based on the expected available aircraft time, target survey speed, and estimated time for circling over detected schools to estimate their size. Aircraft time was allocated to each sub-area in proportion to its area. Transect lines were placed in a north-south direction to be approximately perpendicular to the coast in most blocks and to give shorter transects.

Surveys were designed as equal spaced parallel lines and so that the whole sub-area could be surveyed in two days and then repeated multiple times. The number of 2-day surveys planned for each sub-area was based on the size of the sub-area.

Some changes were made to the original design for logistical reasons. In particular, permission was not given to fly surveys in most of sub-area 4 and this survey effort was redistributed into two new survey sub-areas (7 and 8). Surveys in sub-areas 7 and 8 were designed at ICCAT.

### **Survey coverage**

Figure 1 shows the original designed survey transects for sub-areas 1, 2, 3, 4 and 6 (sub-area 5 was withdrawn). Figures 2, 3 and 4 show the realised transects, the sightings made on and off effort and the effort and sightings together. Figures 5-10 show the planned and realised effort and sightings for each sub-area.

Coverage of sub-areas 1 and 2 was comprehensive. Sub-area 3 was well covered in the north but the southern part (south of  $34^{\circ} 20'$ ) was not surveyed. Sub-area 4 had only a very small amount of survey effort and no results are possible from this area. Sub-area 5 was not surveyed at all. Sub-area 6 was generally well covered but some waters in the north and to the east could not be surveyed. New sub-areas 7 and 8 were well covered. No post-stratification has been undertaken so it is assumed that in sub-areas 3 and 6, the sample density from analysis is representative of the whole area. Analysis with post-stratification for these sub-areas so that estimated density of schools is only extrapolated to the area actually surveyed can readily be undertaken.

### **Data provided**

Draft data collection forms were proposed by Hammond, Cañadas & Vázquez (2010) and modified and generated by ICCAT. The completed data forms were provided electronically to ICCAT and passed on for analysis.

### **Data processing**

There were a number of issues with the data forms that needed to be clarified and/or resolved prior to organising the data into an appropriate form for analysis. These included minor errors/inconsistencies and missing data. Minor errors, etc due to typographical errors were checked with the survey teams, noted and corrected. More significant problems are described below.

Generally, it was clear that there were a number of misunderstandings or differences in interpretation in what was required in several of the data fields. It will be important to resolve these issues prior to conducting another survey.

The most serious problem was with the data on declination angle of each detected school (the angle to a sighted school measured from the horizontal when the school was abeam of (at  $90^{\circ}$  to) the transect line). These data are necessary to calculate the perpendicular distance data that are used to estimate detection probability. No survey team collected these data as intended. However, after discussion with each survey team, direct measurements of perpendicular distance for all BFT sightings for all sub-areas were able to be provided from the difference between the GPS positions on the transect line and over the school. The accuracy of these data is unknown and some were estimated (when the track was not broken). But the data seem to be adequate for analysis. This issue requires further discussion before more surveys are conducted.

When these data were collated, the result of observers not being able to see underneath the aircraft became apparent. As expected, there were few sightings close to the transect line (the width of this gap in the data depended on the sub-area), with the exception of some exactly on the line at zero perpendicular distance. This is not a desirable feature of the data but has been dealt with in analysis, as described below.

The data on school size were not collected consistently on all surveys. This was recorded in some sub-areas as Small, Medium or Large (sub-areas 4, 6, 7 and 8), in another as the estimated size of individual fish (sub-area 1), and in others as the estimated number of fish (sub-areas 2 and 3). Consequently, these data could not be used as a measure of school size in analysis. Data on estimated weight of schools, which were recorded consistently, were used as a measure of school size in analysis.

Data on the identity of which observer(s) was searching on which side of the aircraft were not always complete. After some discussion with the relevant survey teams, these data were able to be completed.

Based on these data, observer levels were created that characterised unique combinations of observers; observer level was used in analysis to investigate the effect of observer on detection probability.

More generally on observer issues, it is understood that the Spotter (main observer) sat in the co-pilot's seat in the front on the right, that (s)he searched on both sides but had a clearer view to the right, and that the Scientist sat in the rear of the aircraft on the left. Thus both sides of the aircraft were searched but not necessarily with equal intensity. This issue requires confirmation and further discussion before more surveys are conducted.

One survey team recorded data on glare only when BFT sightings were made rather than for all searching effort. As a result it was not possible to model detection probability as a function of glare.

Sightings made while the aircraft was transiting to and from the survey area or between transects were mostly attributed to a transect in the data, even though they were not seen on transect. These sightings could be identified as off-effort from the times and were not included in analysis.

In sub-area 8, two preliminary “essai” surveys were undertaken before the main surveys. Three of the six transects in these surveys were outside the defined area so a decision was taken not to include them in analysis. In the same sub-area, four designed transects continued south of the sub-area as defined, including one sighting on effort. This was discovered too late to modify analyses presented here.

Following these investigations and modifications to the data, a combined dataset was created that was consistent across as many data fields as possible. This dataset was entered into software DISTANCE for analysis.

## Data analysis

Analysis of the data followed standard line transect methodology (Buckland *et al.* 2001).

Density of schools was estimated from the number of schools sighted, the length of transect searched and the estimated  $esw$  (reciprocal of the probability of detecting a school within a strip defined by the data). The equation that relates density to the collected data is:

$$\hat{D} = \frac{n \bar{s}}{2 esw L}$$

where  $\hat{D}$  is density (the hat indicates an estimated quantity),  $n$  is the number of separate sightings of schools,  $\bar{s}$  is mean school size (see below),  $L$  is the total length of transect searched, and  $esw$  is the estimated effective strip half-width. The quantity  $2 esw L$  is thus the area of the strip that has been searched. The effective strip half-width is estimated from the perpendicular distance data for all the detected animals. It is effectively the width at which the number of animals detected outside the strip equals the number of animals missed inside the strip, assuming that everything is seen at a perpendicular distance of zero. To calculate the effective strip half-width, we fitted a detection function (see below and Buckland *et al.* 2001 for further details).

Abundance was estimated as:

$$\hat{N} = A \hat{D}$$

where  $A$  is the size of the survey area.

Because school size was measured in tonnes, the final estimate of abundance is the total estimated weight of tunas in the surveyed areas.

All analysis was undertaken in software DISTANCE <http://www.ruwpa.st-and.ac.uk/distance/>, which estimates all quantities and their uncertainties.

### Fitting the detection function

Detection functions were fitted to the perpendicular distance data to estimate the effective strip half-width,  $esw$ . Multi-Covariate Distance Sampling (MCDS) methods were used to allow detection probability to be modelled as a function of covariates additional to perpendicular distance from the

transect line. These covariates were defined in the survey design phase and included sea state, air haziness, water turbidity, observers searching, cue and estimated weight of the school. Table 1 shows the covariates tested in the models.

Analysis could not be done for each sub-area independently because of insufficient sample size. Instead, they were stratified into two sets based on differences and similarities in the data from survey aircraft /teams. One set comprised sub-areas 1 and 3, and the other sub-area comprised sub-areas 2, 4, 6, 7 and 8.

All off effort sightings were discarded for the analysis.

It is common practice to right truncate perpendicular distance data to eliminate sightings at large distances that have no influence on the fit of the detection function close to the transect line (the quantity of interest) but may adversely affect the fit. After initial exploration of the data, different right truncation distances were chosen for each dataset: 7.5 km for sub-areas 1 and 3; and 4.0 km for sub-areas 2, 4, 6, 7 and 8.

In these surveys, lack of downward visibility beneath the aircraft meant that left truncation of the data was also necessary. Left truncation eliminates the area that has not been searched from analysis. For sub-areas 1 and 3, there were several sightings recorded exactly on the transect line (zero perpendicular distance) but then no sightings until  $> 1$  km. Consequently, two analyses are explored: one with no left truncation, and one with truncation at 1.25 km to investigate the effect on results. For sub-areas 2, 4, 6, 7 and 8, the left truncation distance chosen was 0.3 km.

#### *Model diagnostics and selection*

The best functional form (Half Normal or Hazard Rate model) of the detection function and the covariates retained by the best fitting models were selected based on model fitting diagnostics: AIC, goodness of fit tests, Q-Q plots, and inspection of plots of fitted functions.

Q-Q plots (quantile-quantile plots) compare the distribution of two variables; if they follow the same distribution, a plot of the quantiles of the first variable against the quantiles of the second should follow a straight line. To compare the fit of a detection function model to the data, we used a Q-Q plot of the fitted cumulative distribution function (cdf) against the empirical distribution function (edf).

For goodness of fit tests, we used the Kolmogorov-Smirnov statistic (a goodness of fit test that focuses on the largest difference between the cdf and the edf), Cramer-von Mises statistics (that focus on the sum of squared differences between cdf and edf) and the Chi-square goodness of fit statistic (that compares observed with expected frequencies of observations in each selected range of perpendicular distances).

## **Results**

Table 2 shows the area of each survey sub-area, the number and length of searched transects, the number of sightings of bluefin tuna schools and the left and right truncation distances used for analysis.

### **Sub-areas 1 and 3 without left truncation**

The final model selected was a null model (no covariates) with a Hazard-rate key function and no adjustment terms. The Kolmogorov-Smirnov test and the Cramer-von Mises tests performed well and overall there were no significant differences between the cdf and the edf. Nevertheless, the Q-Q plot shows a large disagreement between the cdf and the edf in the first 20% of the data closer to the transect line, also shown by the plot of the detection function, where there is a big gap in detections between close to the transect line and 1.25 km from the transect line. Table 3 shows the main parameters for the detection function and the results of the diagnostics tests. Figure 11 shows the fitted detection function and Figure 12 shows the Q-Q plot.

Table 4 shows the estimates of density of schools, mean school size and total weight of bluefin tuna in each sub-area.

### **Sub-areas 1 and 3 with left truncation**

The final model selected was a null model (no covariates) with a Hazard-rate key function and no adjustment terms. The Kolmogorov-Smirnov test and the Cramer-von Mises tests performed well, better than with no left truncation, and overall there were no significant differences between the cdf and the edf.

The Q-Q plot shows a much better agreement between the cdf and the edf in 20% of the data closer to the transect line. Table 3 shows the main parameters for this detection function and the results of the diagnostics tests. Figure 13 shows the fitted detection function and Figure 14 shows the Q-Q plot.

Table 5 shows the estimates of density of schools, mean school size and total weight of bluefin tuna in each sub-area.

Based on the better fit of the detection function, we selected these results as the best estimates for sub-areas 1 and 3.

### **Sub-areas 2, 4, 6, 7 and 8**

The final model selected was a null model (no covariates) with a Hazard-rate key function and no adjustment terms. The Kolmogorov-Smirnov test and the Cramer-von Mises tests performed very well, and overall there were no significant differences between the cdf and the edf. The Q-Q plot shows a very good fit between the cdf and the edf. Table 3 shows the main parameters for this detection function and the results of the diagnostics tests. Figure 15 shows the fitted detection function and Figure 16 shows the Q-Q plot.

Table 6 shows the estimates of density of schools and total weight of bluefin tuna in each sub-area.

### **All sub-areas**

Table 7 pulls together the results for all sub-areas and shows results for all sub-areas combined. Overall, a total of 18,158 (CV = 33%) tonnes of bluefin tuna was estimated in the six sub-areas.

## **Discussion**

### **Survey logistics**

The survey design generally seemed to function as planned. Evenly spaced north-south transects seemed to work well as a design configuration. Completing a survey over 2 days also seems effective. Further discussion of logistical issues relating to the survey will best be achieved with ICCAT and the survey teams.

### **Precision of estimates**

The CV of abundance is determined by the CVs of estimated density of schools and mean school sizes in each sub-area. The CV of estimated density of schools is determined by the CVs of encounter rate (number of schools seen per survey km) and effective strip half width ( $esw$ ). All of these quantities are functions of the number of schools seen, as well as the distribution of the data.

The achieved precision (CV) of the estimates for each sub-area are summarised in Table 8.

The number of schools seen in sub-areas 1, 2, 7 and 8 was small (<10) which lead to CVs for density of schools of >50%. However, even where sample size was higher in sub-areas 3 and 6 (around 20-30 schools), the CV of density of schools was still no better than 40%. The precision of mean school size was generally smaller (CV of 6-25% in sub-areas 1, 2, 3 and 6) but greater than 50% in sub-areas 7 and 8, where there were few sightings. CVs for estimates of total abundance in each sub-area were high: 40-60% in sub-areas 1, 2, 3 and 6; and greater than 90% in sub-areas 7 and 8. Summing over all sub-areas surveyed, the CV of total abundance was 33%.

The number of schools seen in several sub-areas was insufficient to estimate an independent  $esw$  so data from sub-areas surveyed by the same team were pooled. This is acceptable as long as differences in conditions in each sub-area (such as sea state, air haziness, water turbidity, observers) can be investigated as a covariate in fitting the detection function. Using the same  $esw$  for multiple sub-areas generates correlation in the estimates which was taken into account (in software DISTANCE) in estimating the CV of total abundance.

Inspection of Figures 5-10 shows that in most sub-areas the distribution of sightings was quite aggregated, which increases the CV of estimated density of schools. Incorporating the CV of mean school size made relatively little difference to the CV of estimated abundance.

The main way to reduce the estimated CVs in future surveys is to increase the number of sightings. This can be achieved partly by more efficient searching (for example, using aircraft with good downward visibility) and partly by increasing the amount of searching effort (transect length). Using aircraft with bubble windows would increase sample size and also avoid the need to left truncate the perpendicular distance data.

Increasing searching effort will lead to a decrease in CV of abundance but it is not possible to make exact predictions about how much. CV should improve approximately as a function of the square root of sample size, as shown in Hammond, Cañadas & Vázquez (2010). As a rough idea of the effect, if total sample size were doubled from 72 sightings to 144 sightings by improving efficiency of searching beneath the aircraft and/or increasing searching effort, we might expect the CV of total abundance to decrease from 0.33 to about 0.24.

### **Relative estimates of abundance**

Line transect sampling assumes that detection on the transect line itself is certain. On aerial surveys, in general, it is not possible to assume this because the speed of flight means that some schools available to be sampled will inevitably not be detected (so-called perception bias). In addition, tuna spend much of their time beneath the surface and unavailable to be detected (so-called availability bias). Estimates of abundance from these surveys are thus underestimates (minimum estimates) even though a detection function has been fitted to correct for animals missed within the survey strip.

The appropriateness of these estimates as indices of abundance for the future depends on a number of factors including: timing of surveys; areas surveyed; and stability of availability and perception biases. Availability and perception bias can reasonably be assumed to be stable over time but knowledge of the distribution in time and space of bluefin tuna throughout the Mediterranean Sea is incomplete. To minimise natural variation in using survey estimates as indices of abundance over time, surveys in future years should ideally occur in the same areas at the same time of year.

### **Power to detect trends**

The power of the data to detect trends in abundance depends on a number of factors: the number of years of surveying; the CV of the abundance estimates; the direction and magnitude of the trend; and the probability of a Type I error (rejecting the null hypothesis when it is actually true). Power is defined as one minus the probability of a Type II error (accepting the null hypothesis when it is actually false). The probability of a Type I error is usually referred to as  $\alpha$ . The probability of a Type II error is usually referred to as  $\beta$ ; hence power =  $1 - \beta$ . The conventional value for acceptable power is 0.8.

We used software TRENDS (Gerrodette, 1987) to investigate the relationship between power, the estimated CV of total abundance, the number of survey years, and rate of population change per year. Specifically, the following were investigated:

- (a) the power of the data to detect a trend (annual rate of population change) of given magnitude as a function of the number of survey years;
- (b) the annual rate of population change detectable if CV of abundance were improved as a function of the number of survey years;
- (c) the CV of abundance needed in future surveys to detect a trend of given magnitude as a function of the number of survey years.

Results are given in Tables 9, 10 and 11. Table 9 shows that the power of the data (CV of abundance of 0.33) from these surveys to detect a declining trend of 5% per year is very low, even after 10 years. Power to detect a declining trend of 10% per year reaches 0.8 after 9 years of surveys and after only 6 years if the trend is a decline of 20% per year.

The magnitude of the trend detectable declines as the CV of abundance decreases and the number of survey years increases (Table 10), but this result is not particularly sensitive to the size of the CV. For example, after 7 years of survey, the trend detectable is -0.14 with CV=0.33, -0.11 with CV=0.25, and -0.09 with CV=0.20. Or, considered another way, to detect an annual trend of 10% would take 9 years with CV=0.33, 8 years with CV=0.25, and 7 years with CV=0.20.

With the current CV of 0.33, a 5% annual decline would take 14 years to detect, a 10% annual decline 9 years, and a 20% annual decline 6 years (Table 11). The CV of abundance necessary to detect a trend of given magnitude declines fairly linearly with the number of survey years.

## **Recommendations**

### **Future survey design**

Parallel, equal spaced, N-S transects on surveys run over two days generally seems a good design. Other features that would improve the effectiveness of the surveys include:

- Use aircraft with good downward visibility (including bubble windows for rear observers);
- Review data collection forms and tighten up the descriptions of data required;
- Hold a training workshop with all survey teams to ensure consistent understanding of data collection;
- Observers to use inclinometers to measure declination angle of schools when abeam;

### **Data analysis**

- If data on other species (cetaceans, turtles) could be collected with the same rigour as those on bluefin tuna, this would be extremely cost-efficient and would contribute greatly to cetacean and turtle research and conservation issues in the Mediterranean Sea;
- If a greater amount of more rigorously collected data can be obtained, there is a possibility of using habitat modelling to predict abundance as a function of environment features such as sea surface temperature and chlorophyll concentration.

## **References**

- Buckland, ST, Anderson, DR, Burnham, KP, Laake, JL, Borchers, DL & Thomas, L (2001). *Introduction to distance sampling: estimating abundance of biological populations*. Oxford University Press, Oxford.
- Gerrodette, T (1987). A power analysis for detecting trends. *Ecology* 68: 1364-72. Software TRENDS available from <http://swfsc.noaa.gov/textblock.aspx?Division=PRD&ParentMenuId=228&id=4740>.
- Hammond, Cañadas & Vázquez (2010). Atlantic-wide research programme on bluefin tuna (GBYP - 2010) - Design for aerial line transect survey in the Mediterranean Sea. Final Report to ICCAT. May 2010.

**Table 1.** Areas, number and total length of transects and number of sightings of bluefin tuna for each survey sub-area. Truncation distances are shown for each set of sub-areas.

Sub-area	Area (km <sup>2</sup> )	Number of transects	Length of transects (km)	Number of observations (after truncation)	Left truncation (km)	Right truncation (km)
<b>1 &amp; 3</b>					0	7.5
1	62,263	52	6,301.4	11		
3	90,796	42	5,288.4	23		
Subtotal 1 & 3	163,059	94	11,589.8	34		
<b>1 &amp; 3</b>					1.25	7.5
1	62,263	52	6,301.4	7		
3	90,796	42	5,288.4	19		
Subtotal 1 & 3	163,059	94	11,589.8	26		
<b>2, 4, 6, 7 &amp; 8</b>					0.3	4.0
2	52,461	45	8,702.6	6		
4	74,313					
6	55,248	55	3,482.0	31		
7	19,863	29	2,994.6	3		
8	16,842	22	4,109.9	6		
Subtotal 2, 4, 6, 7 & 8	218,513	157	19,289.1	46		
<b>Total</b>	<b>381,572</b>	<b>251</b>	<b>30,878.9</b>	<b>72</b>		

**Table 2.** Covariates tested in the models and their ranges or factor levels

Covariate	Type	Range	Levels
<b>Sighting related</b>			
Cue	factor		ripples shining splash travelling other
School size	continuous	8 -750 tonnes	
<b>Effort related</b>			
Beaufort sea state	factor		0 to 4 clear slight medium heavy
Air haziness	factor		clear slight medium heavy
Water turbidity	factor		clear slight medium heavy
Observer level	factor		1 to 7

**Table 3.** Parameters and diagnostics of the detection functions.

Sub-areas	Average probability of detection (p)	Effective strip width (esw) (km)	K-S test (p)	Cramer-von Mises test (uniform weighting) (p)	Cramer-von Mises test (cosine weighting) (p)
<b>1 and 3</b> with left truncation	0.644	4.8301	0.112	0.150 < p <= 0.200	0.100 < p <= 0.150
<b>1 and 3</b> without left truncation	0.471	3.5343	0.198	0.200 < p <= 0.300	0.200 < p <= 0.300
<b>2, 4, 6, 7 and 8</b>	0.364	1.4577	0.900	0.900 < p <= 1.000	0.900 < p <= 1.000

**Table 4.** Mean school size, density of schools and total weight of bluefin tuna in sub-areas 1 and 3, using the detection function without left truncation.

No left truncation		Sub-area		
		1	3	1 and 3
<b>Number of transects</b>		52	42	<b>94</b>
<b>Transect length (km) (L)</b>		6,301.4	5,288.4	<b>11,589.8</b>
<b>Number of sightings (n)</b>		11	23	<b>34</b>
<b>School size (tonnes)</b>	<b>Mean school size</b>	129.1	41.8	
	<b>CV (%)</b>	8.45	26.3	
<b>Density of schools (km<sup>-2</sup>)</b>	<b>Density of schools</b>	0.00018	0.00045	<b>0.00034</b>
	<b>CV (%)</b>	47.3	38.3	<b>32.7</b>
	<b>Lower 95% CL</b>	0.00007	0.00021	<b>0.00018</b>
	<b>Upper 95% CL</b>	0.00044	0.00095	<b>0.00064</b>
<b>Total weight (tonnes)</b>	<b>Total weight</b>	1,453	1,709	<b>3,162</b>
	<b>CV (%)</b>	48	47	<b>35</b>
	<b>Lower 95% CL</b>	584	708	<b>1,620</b>
	<b>Upper 95% CL</b>	3,610	4,125	<b>6,170</b>
<b>Encounter rate of schools (1,000 km<sup>-1</sup>)</b>	<b>n/L</b>	1.75	4.35	<b>2.93</b>
	<b>CV (%)</b>	45.2	35.7	

**Table 5.** Mean school size, density of schools and total weight of bluefin tuna in sub-areas 1 and 3, using the detection function with left truncation.

Left truncation	Sub-area			
	1	3	1 and 3	
Number of transects	52	42	<b>94</b>	
Transect length (km) (L)	6,301.4	5,288.4	<b>11,589.8</b>	
Number of sightings (n)	11	23	<b>34</b>	
School size (tonnes)	Mean school size	127.1	50.6	
	CV (%)	8.00	24.6	
Density of schools (km <sup>-2</sup> )	Density of schools	0.00016	0.00051	<b>0.00037</b>
	CV (%)	55.0	44.1	<b>39.2</b>
	Lower 95% CL	0.00006	0.00022	<b>0.00017</b>
	Upper 95% CL	0.00044	0.00118	<b>0.00078</b>
Total weight (tonnes)	Total weight	1,244	2,335	<b>3,579</b>
	CV (%)	55.6	50.5	<b>40.6</b>
	Lower 95% CL	442	905	<b>1,652</b>
	Upper 95% CL	3,506	6,030	<b>7,759</b>
Encounter rate of schools (1,000 km <sup>-1</sup> )	n/L	1.11	3.59	<b>2.24</b>
	CV (%)	51.1	39.0	

**Table 6.** Mean school size, density of schools and total weight of bluefin tuna in sub-areas 2, 6, 7 and 8.

		Sub-area				
		2	6	7	8	2, 6, 7, 8
<b>Number of transects</b>		45	55	29	22	<b>151</b>
<b>Transect length (km) (L)</b>		8,702.6	3,482.0	2,994.6	4,109.9	<b>19,289.1</b>
<b>Number of sightings (n)</b>		6	31	3	6	<b>46</b>
<b>School size (tonnes)</b>	<b>Mean school size</b>	124.2	62.1	19.2	293.3	
	<b>CV (%)</b>	5.6	12.9	67.5	50.6	
<b>Density of schools (km<sup>-2</sup>)</b>	<b>Density of schools</b>	0.00024	0.00305	0.00034	0.00050	<b>0.00136</b>
	<b>CV (%)</b>	52.6	39.8	61.9	77.6	<b>38.0</b>
	<b>Lower 95% CL</b>	0.00009	0.00142	0.00011	0.00012	<b>0.00065</b>
	<b>Upper 95% CL</b>	0.00063	0.00655	0.00118	0.00204	<b>0.00282</b>
<b>Total weight (tonnes)</b>	<b>Total weight</b>	1,541	10,434	131	2,474	<b>14,579</b>
	<b>CV (%)</b>	52.9	41.9	91.6	92.6	<b>40.1</b>
	<b>Lower 95% CL</b>	574	4,702	20	495	<b>6,777</b>
	<b>Upper 95% CL</b>	4,137	23,152	849	12,374	<b>31,362</b>
<b>Encounter rate of schools (1,000 km<sup>-1</sup>)</b>	<b>n/L</b>	0.69	8.90	1.00	1.46	<b>2.38</b>
	<b>CV (%)</b>	42.5	25.0	53.5	71.1	

**Table 7.** Summary of estimates for all sub-areas.

<b>Sub-area</b>	<b>1</b>	<b>2</b>	<b>3</b>	<b>6</b>	<b>7</b>	<b>8</b>	<b>Total</b>
<b>Survey area (km<sup>2</sup>)</b>	62,264	52,461	90,796	55,034	19,863	16,842	<b>297,260</b>
<b>Number of transects</b>	52	45	42	55	29	22	<b>245</b>
<b>Transect length (km)</b>	6,301.4	8,702.6	5,288.4	3,482.0	2,994.6	4,109.9	<b>30,878.9</b>
<b>Effective strip width x 2 (km)</b>	7.069	2.915	7.069	2.915	2.915	2.915	
<b>Area searched (km<sup>2</sup>)</b>	44,542.1	25,371.6	37,381.6	10,151.4	8,730.5	11,982.0	<b>138,159.1</b>
<b>% coverage</b>	71.5	48.4	41.2	18.4	44.0	71.1	
<b>Number of schools</b>	7	6	19	31	3	6	<b>72</b>
<b>Density of schools (1000 km<sup>-2</sup>)</b>	0.157	0.236	0.508	3.054	0.344	0.501	<b>0.521</b>
<b>%CV density of schools</b>	55.0	52.6	44.1	39.8	61.9	77.6	
<b>Mean school size (t)</b>	127.1	124.2	50.6	62.1	19.2	293.3	<b>88.0</b>
<b>%CV school size</b>	8.0	5.6	2.5	12.9	67.5	50.6	
<b>Total weight (t)</b>	<b>1,244</b>	<b>1,541</b>	<b>2,335</b>	<b>10,434</b>	<b>131</b>	<b>2,474</b>	<b>18,158</b>
<b>%CV total weight</b>	55.6	52.9	50.5	41.9	91.6	92.6	<b>33.0</b>

**Table 8.** CVs for density of schools, mean school size and total weight.

Sub-area	Number of schools	Density of schools (1000 km <sup>-2</sup> )	%CV density of schools	Mean school size (t)	%CV mean school size	Total weight (t)	%CV total weight
1	7	0.157	55.0	127.1	8.0	1,244	55.6
2	6	0.236	52.6	124.2	5.6	1,541	52.9
3	19	0.508	44.1	50.6	2.5	2,335	50.5
6	31	3.054	39.8	62.1	12.9	10,434	41.9
7	3	0.344	61.9	19.2	67.5	131	91.6
8	6	0.501	77.6	293.3	50.6	2,474	92.6
<b>All</b>	<b>72</b>	<b>0.521</b>		<b>88.0</b>		<b>18,158</b>	<b>33.0</b>

**Table 9.** Power of the data to detect a trend as a function of the magnitude of the trend (annual rate of population change) and the number of years of survey.  $\alpha = 0.05$ . CV of abundance = 0.33.

Annual rate of population change	Number of survey years	Power to detect trend (1 - $\beta$ )
-0.05	4	0.09
	5	0.11
	6	0.14
	7	0.19
	8	0.25
	9	0.32
	10	0.42
-0.10	4	0.14
	5	0.21
	6	0.34
	7	0.50
	8	0.69
	9	0.86
	10	0.96
-0.20	4	0.30
	5	0.60
	6	0.90
	7	0.99
	8	1.00
	9	1.00
	10	1.00

**Table 10.** The annual rate of population change (trend) detectable as a function of the CV of abundance and the number of years of survey.  $\alpha = 0.05$ . Power  $(1 - \beta) = 0.80$ .

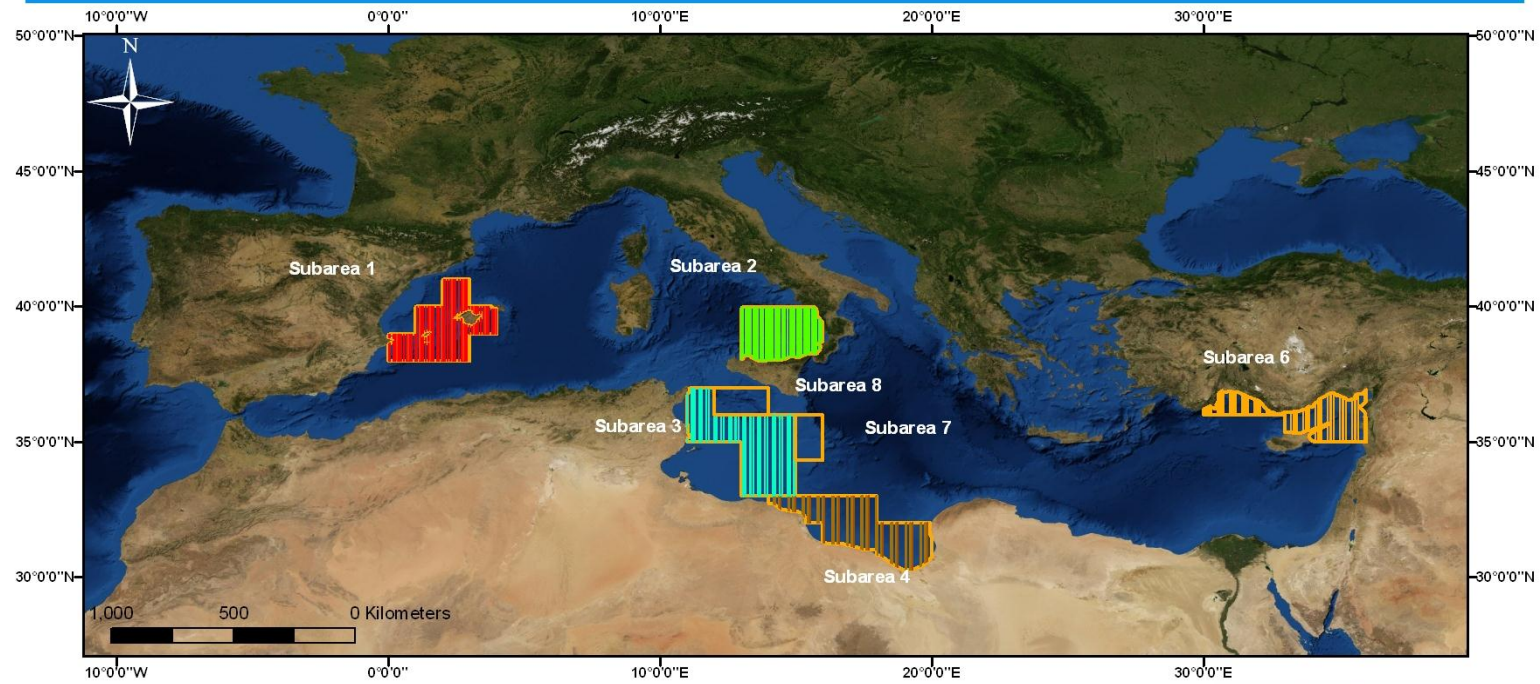
<b>CV of abundance</b>	<b>Number of survey years</b>	<b>Annual rate of population change</b>
0.33	4	-0.44
	5	-0.25
	6	-0.18
	7	-0.14
	8	-0.11
	9	-0.09
	10	-0.08
0.25	4	-0.32
	5	-0.20
	6	-0.15
	7	-0.11
	8	-0.09
	9	-0.07
	10	-0.06
0.20	4	-0.27
	5	-0.17
	6	-0.12
	7	-0.09
	8	-0.07
	9	-0.06
	10	-0.05

**Table 11.** The CV of abundance needed to detect a given annual rate of population change (trend) as a function of the number of survey years.  $\alpha = 0.05$ . Power  $(1 - \beta) = 0.80$ .

<b>Annual rate of population change</b>	<b>Number of survey years</b>	<b>CV of abundance</b>
-0.05	14	0.33
	13	0.30
	12	0.26
	11	0.21
	10	0.18
	9	0.15
	-0.10	9
8		0.28
7		0.21
6		0.15
-0.20	6	0.33
	5	0.24
	4	0.13


**ICCAT**

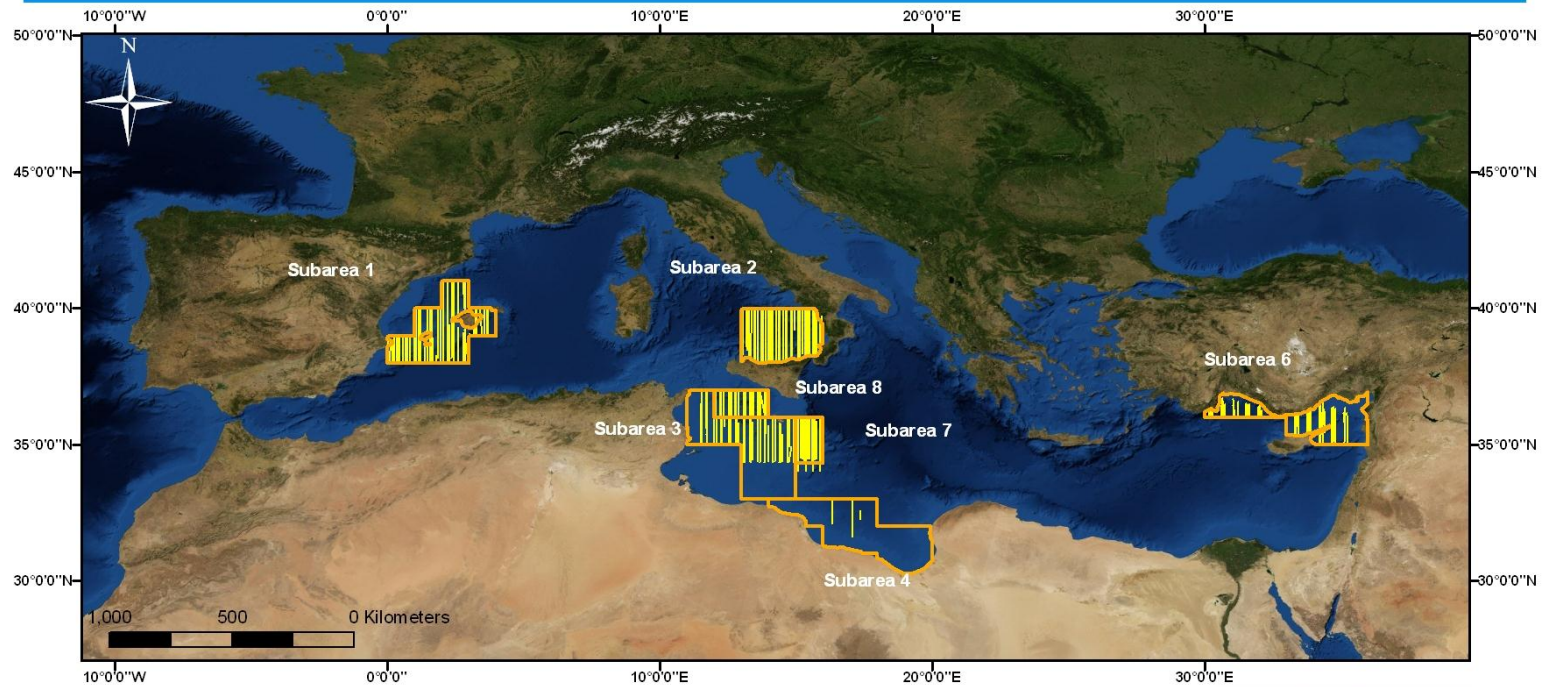
**ATLANTIC-WIDE RESEARCH PROGRAMME ON BLUEFIN TUNA (ICCAT/GBYP – 2010)**  
**2010 Aerial Survey on Spawning Aggregations**

***Designed Transects 2010***



**Figure 1.** Originally designed transects for sub-areas 1, 2, 3, 4 and 6 (after Hammond *et al.* 2010).



***Covered Transects 2010***



**Figure 2.** Transects flown on effort in sub-areas 1, 2, 3, 4, 6, 7 and 8.

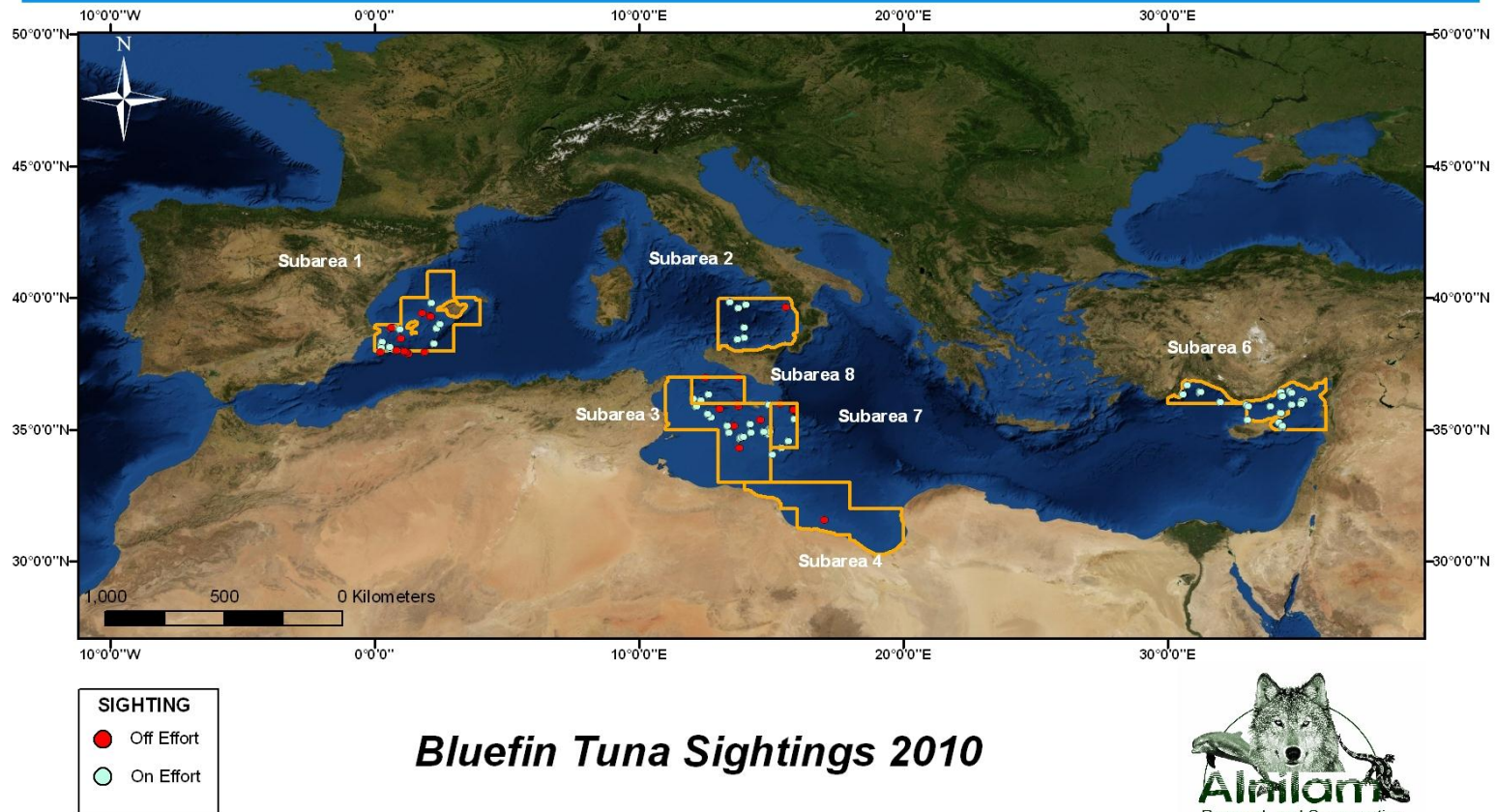
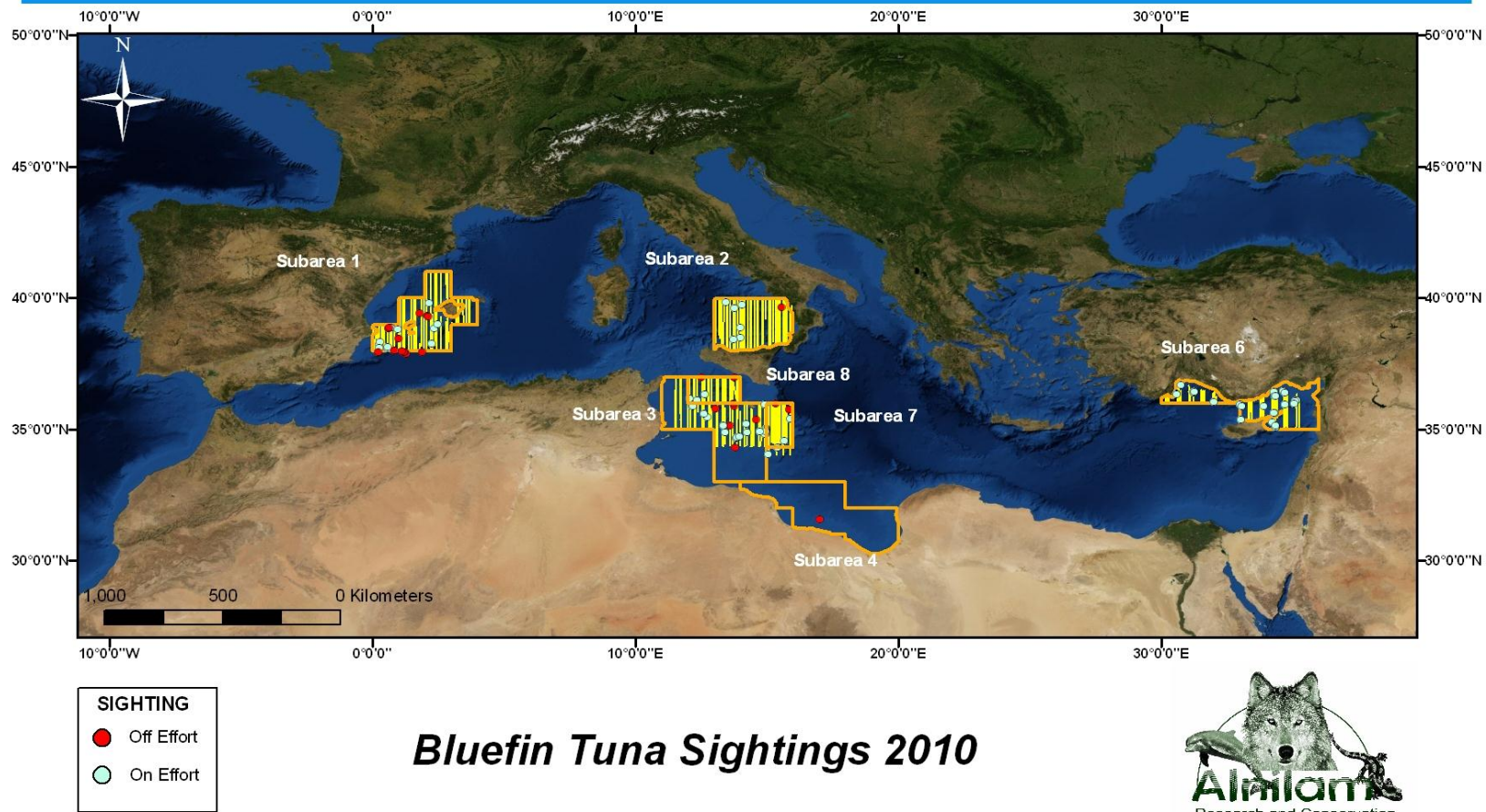


Figure 3. Sightings of bluefin tuna on and off effort in sub-areas 1, 2, 3, 4, 6, 7 and 8.



**Bluefin Tuna Sightings 2010**

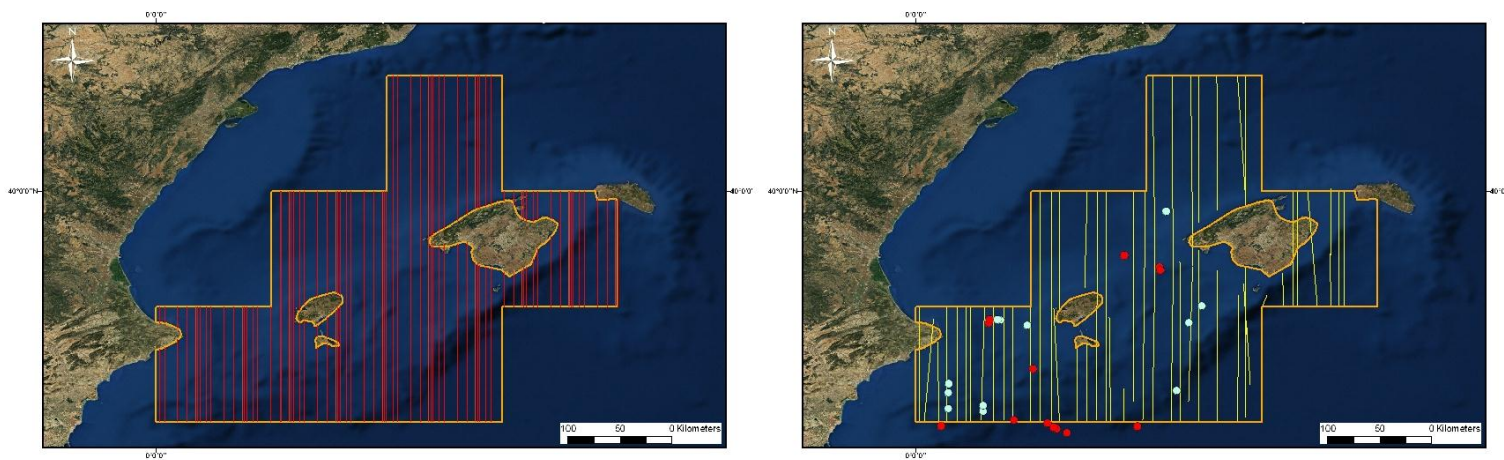
**Figure 4.** Transects flown and sightings of bluefin tuna on and off effort in sub-areas 1, 2, 3, 4, 6, 7 and 8.



ICCAT

# ATLANTIC-WIDE RESEARCH PROGRAMME ON BLUEFIN TUNA (ICCAT/GBYP – 2010)

## 2010 Aerial Survey on Spawning Aggregations



SIGHTING	TRANSECT
● Off Effort	— Designed
○ On Effort	— Covered

### *Bluefin Tuna Sightings 2010 Subarea 1*



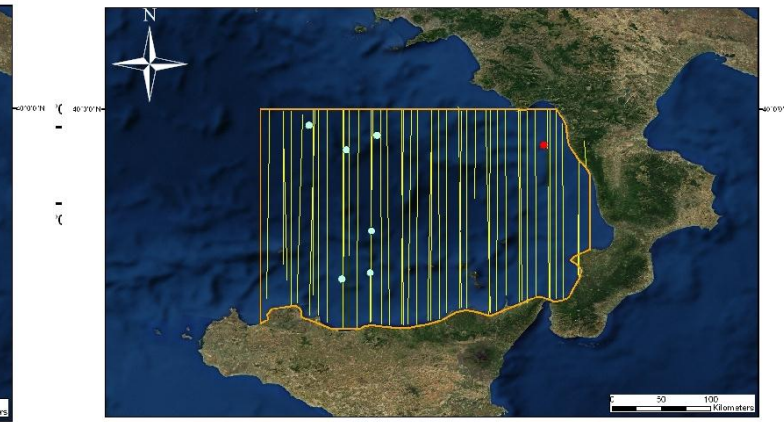
**Figure 5.** Transects designed and flown, and sightings of bluefin tuna on and off effort in sub-area 1.



ICCAT

# ATLANTIC-WIDE RESEARCH PROGRAMME ON BLUEFIN TUNA (ICCAT/GBYP – 2010)

## 2010 Aerial Survey on Spawning Aggregations



SIGHTING	TRANSECTS
<span style="color: red;">●</span> Off Effort	<span style="color: green;">—</span> Designed
<span style="color: blue; border: 1px solid blue; border-radius: 50%; padding: 2px;">●</span> On Effort	<span style="color: yellow;">—</span> Covered

### *Bluefin Tuna Sightings 2010 Subarea 2*



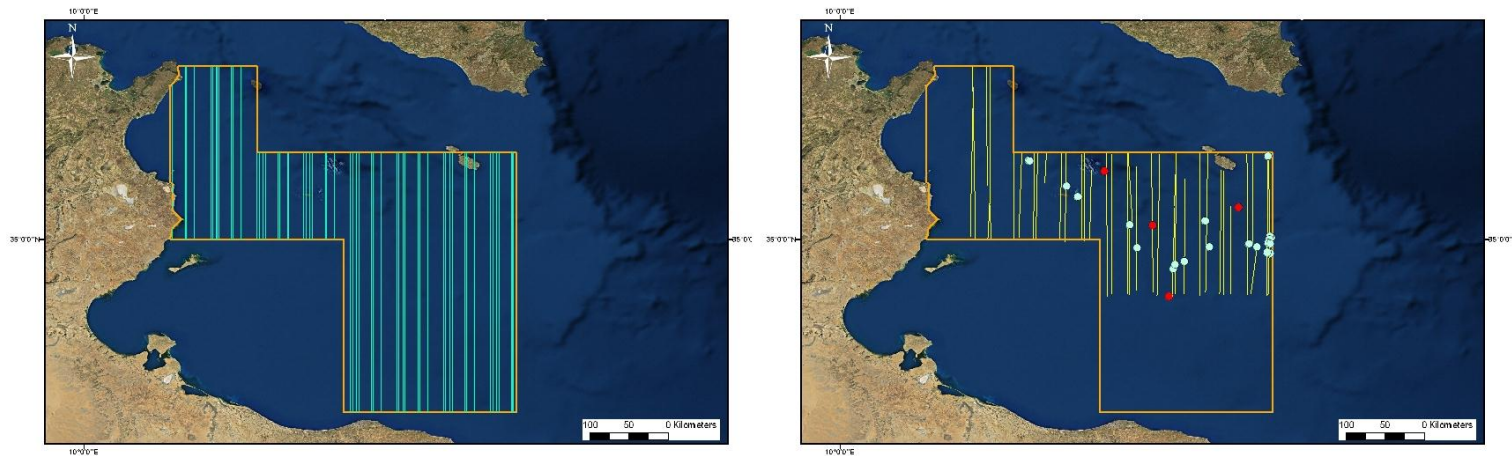
**Figure 6.** Transects designed and flown, and sightings of bluefin tuna on and off effort in sub-area 2.



ICCAT

# ATLANTIC-WIDE RESEARCH PROGRAMME ON BLUEFIN TUNA (ICCAT/GBYP – 2010)

## 2010 Aerial Survey on Spawning Aggregations



### *Bluefin Tuna Sightings 2010 Subarea 3*



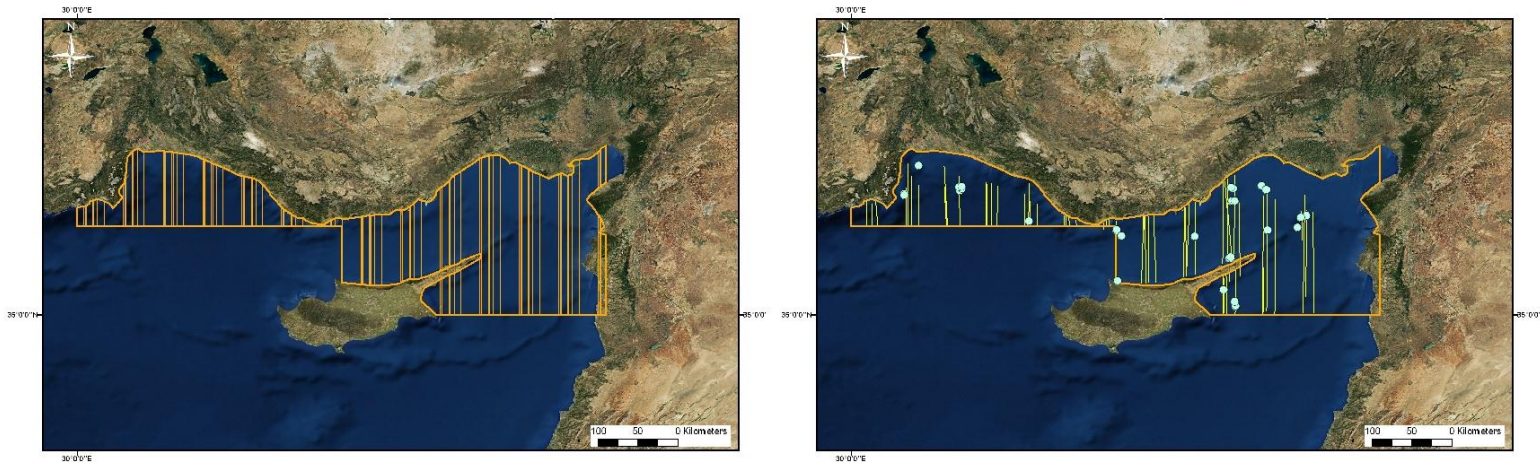
**Figure 7.** Transects designed and flown, and sightings of bluefin tuna on and off effort in sub-area 3.



ICCAT

# ATLANTIC-WIDE RESEARCH PROGRAMME ON BLUEFIN TUNA (ICCAT/GBYP – 2010)

## 2010 Aerial Survey on Spawning Aggregations



SIGHTING		TRANSECT	
<span style="color: red;">●</span>	Off Effort	<span style="color: orange;">—</span>	Designed
<span style="color: lightblue;">●</span>	On Effort	<span style="color: yellow;">—</span>	Covered

### *Bluefin Tuna Sightings 2010 Subarea 6*



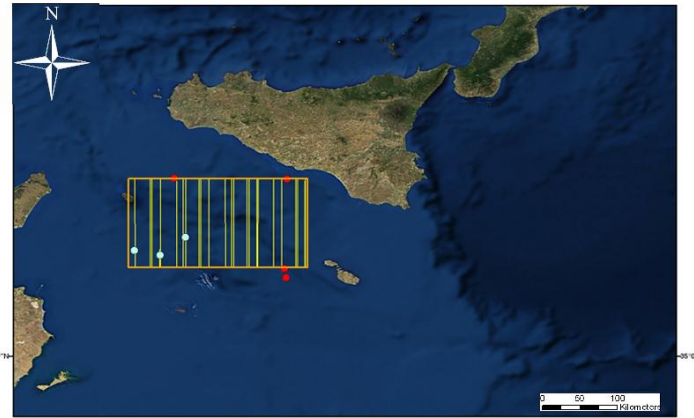
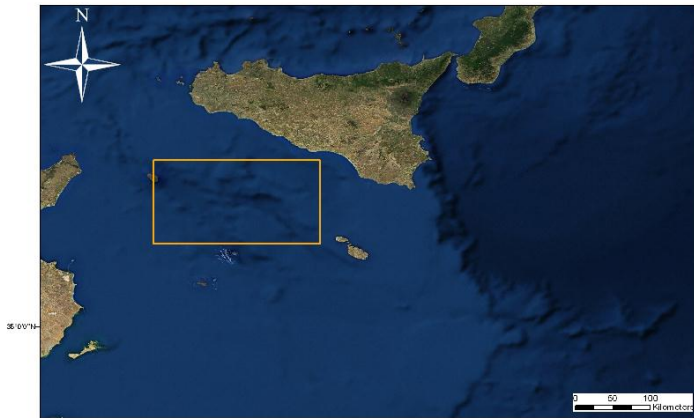
**Figure 8.** Transects designed and flown, and sightings of bluefin tuna on and off effort in sub-area 6.



ICCAT

# ATLANTIC-WIDE RESEARCH PROGRAMME ON BLUEFIN TUNA (ICCAT/GBYP – 2010)

## 2010 Aerial Survey on Spawning Aggregations



SIGHTING	TRANSECTS
<span style="color: red;">●</span> Off Effort	<span style="color: yellow;">—</span> Designed
<span style="color: green;">●</span> On Effort	<span style="color: yellow;">—</span> Covered

### *Bluefin Tuna Sightings 2010 Subarea 7*



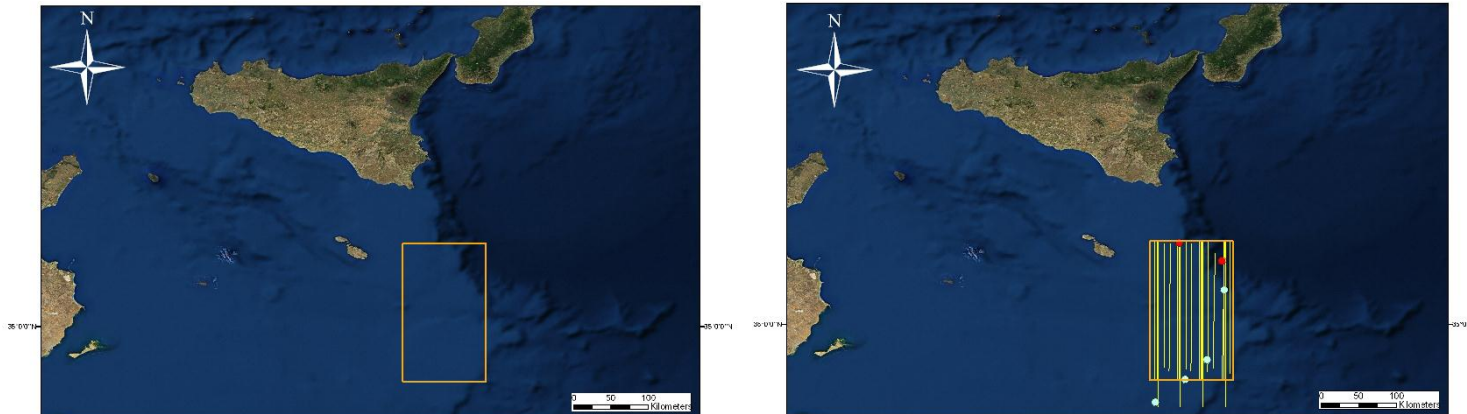
**Figure 9.** Transects designed and flown, and sightings of bluefin tuna on and off effort in sub-area 7.



ICCAT

# ATLANTIC-WIDE RESEARCH PROGRAMME ON BLUEFIN TUNA (ICCAT/GBYP – 2010)

## 2010 Aerial Survey on Spawning Aggregations



SIGHTING	TRANSECTS
● Off Effort	— Designed
● On Effort	— Covered

### *Bluefin Tuna Sightings 2010 Subarea 8*



**Figure 10.** Transects designed and flown, and sightings of bluefin tuna on and off effort in sub-area 8.

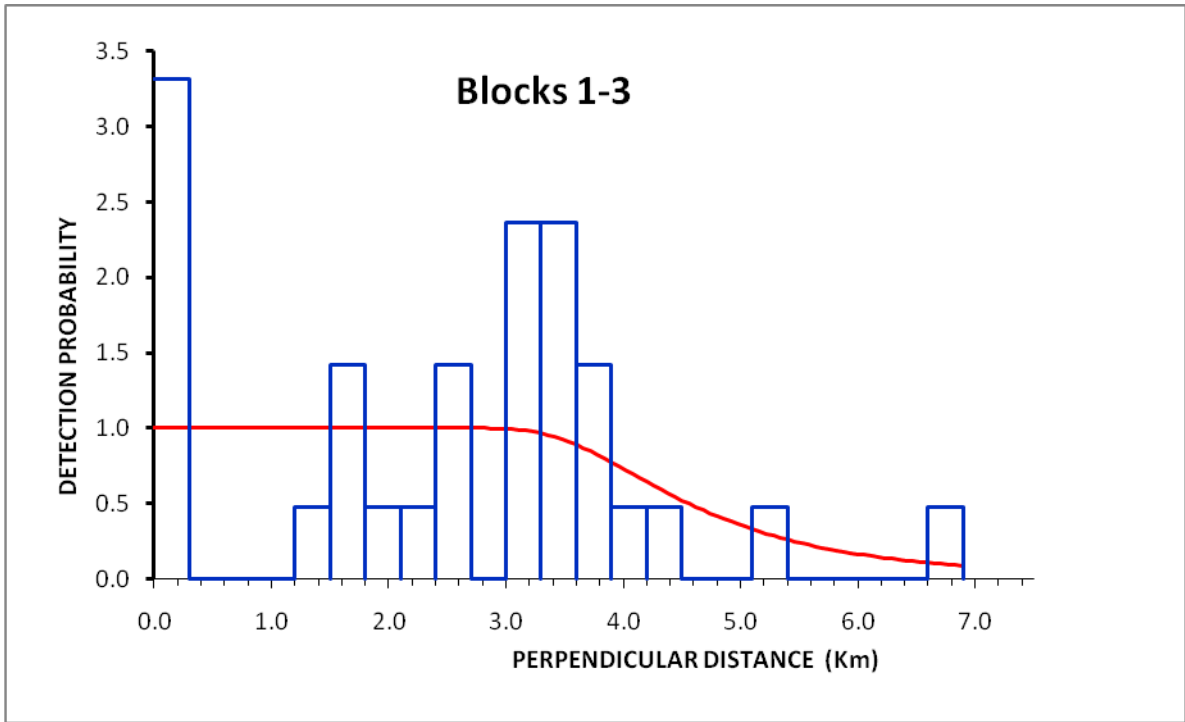


**Figure 11.** Detection function for sub-areas 1-3 without left truncation, scaled to 1.0 at zero perpendicular distance, and histograms of observed sightings.

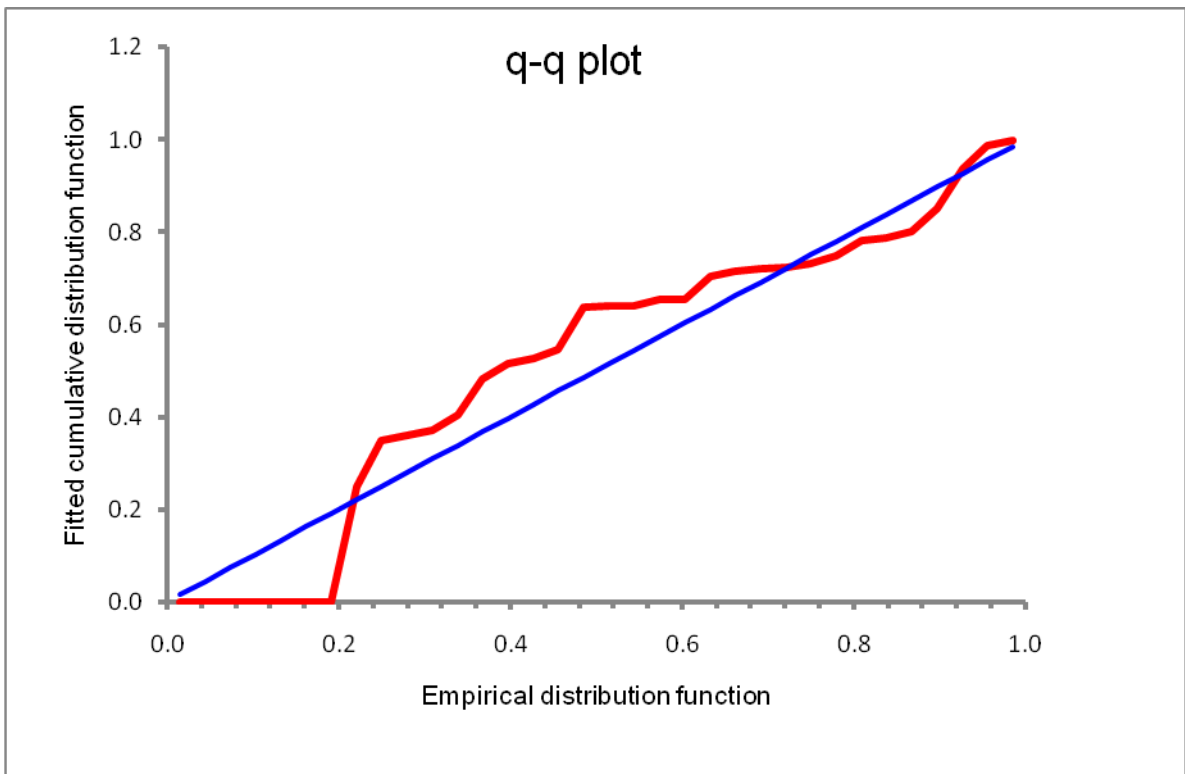


**Figure 12.** Q-Q plot for sub-areas 1-3 with no left truncation

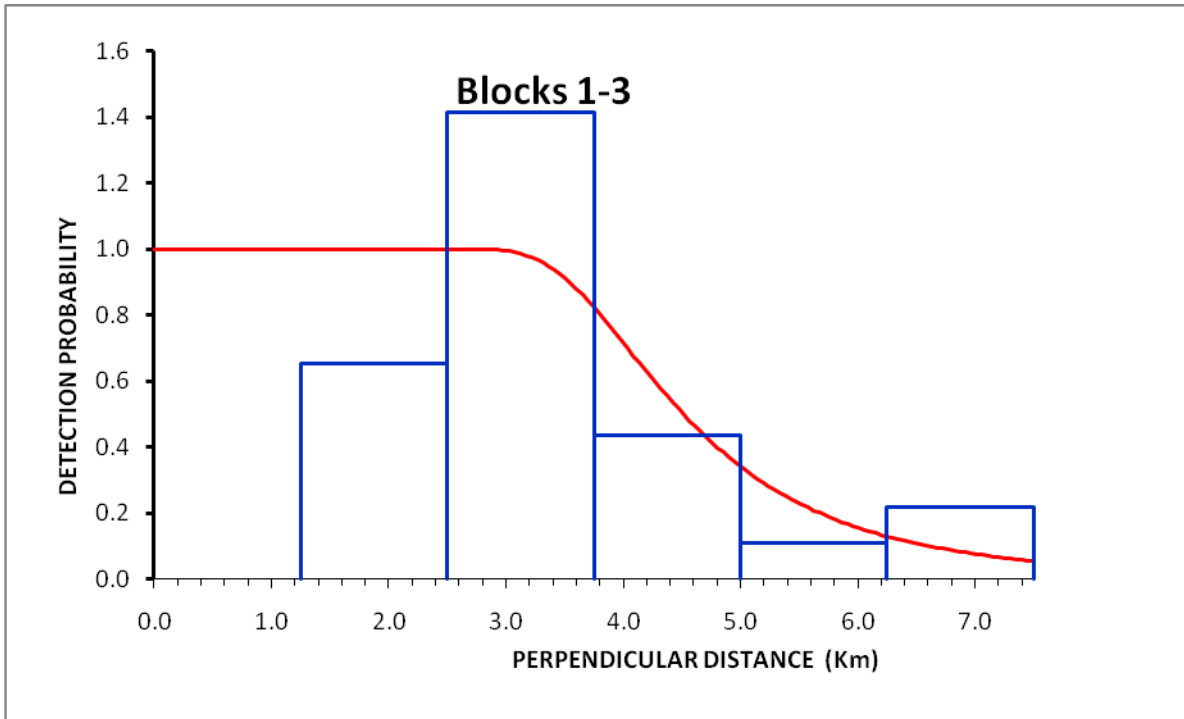


**Figure 13.** Detection function for sub-areas 1-3 with left truncation at 1.25km, scaled to 1.0 at zero perpendicular distance, and histograms of observed sightings.

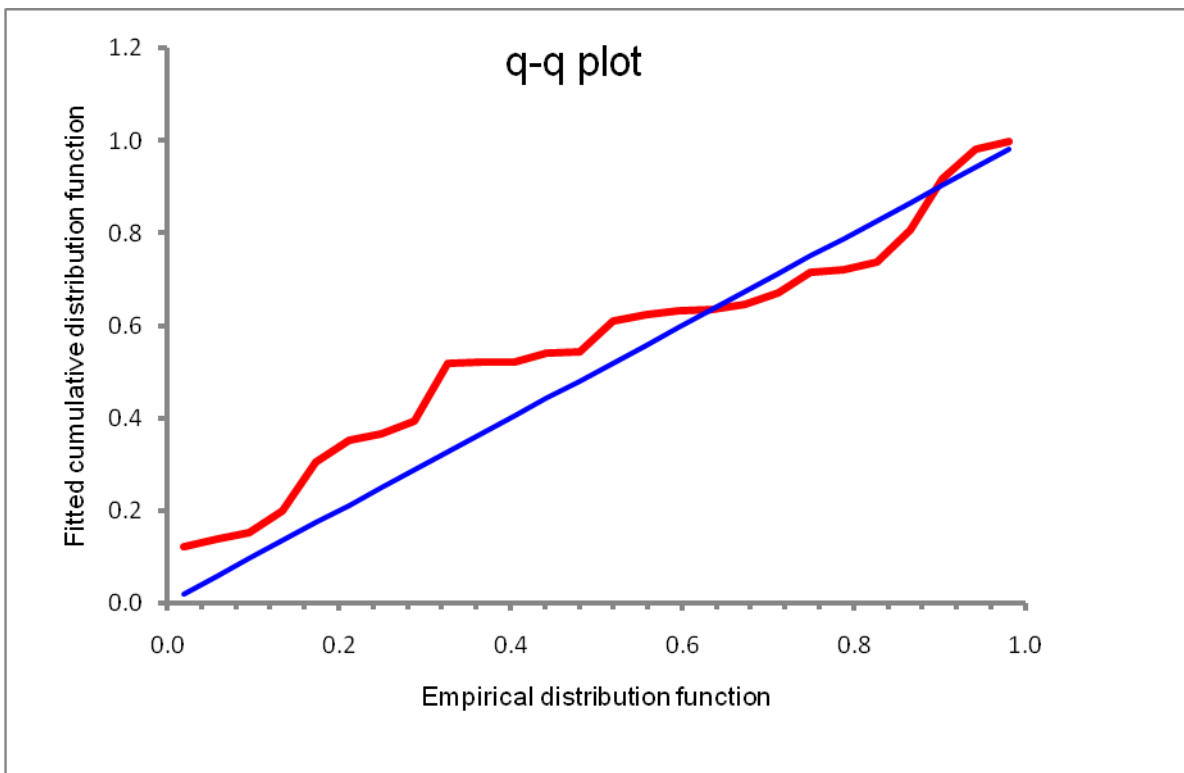


**Figure 14.** Q-Q plot for sub-areas 1-3 with left truncation

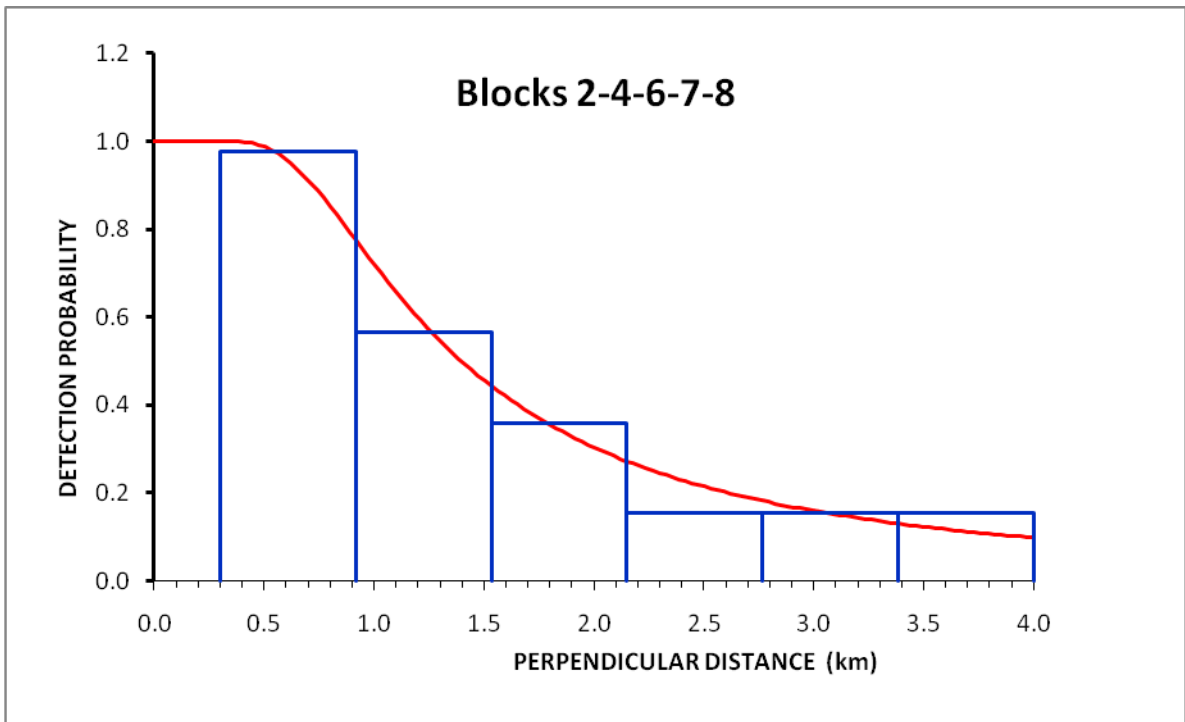


**Figure 15.** Detection function for sub-areas 2, 4, 6, 7 and 8, scaled to 1.0 at zero perpendicular distance, and histograms of observed sightings.

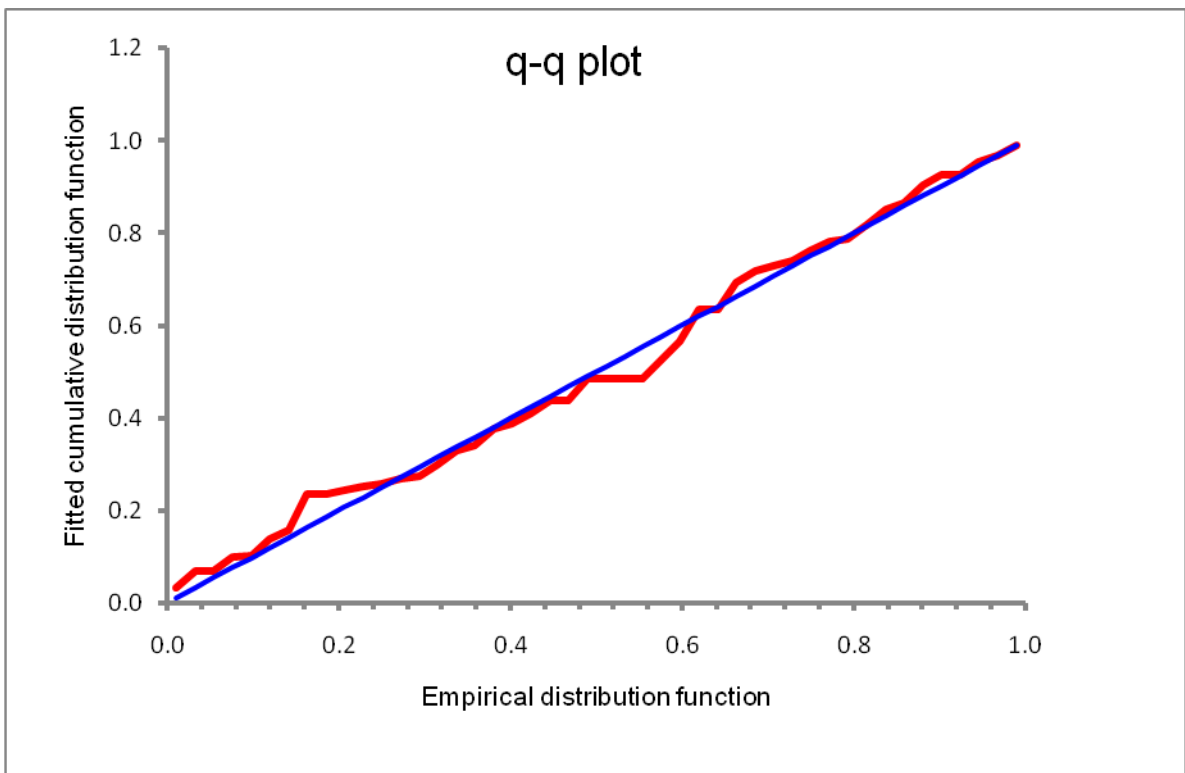


**Figure 16.** Q-Q plot for sub-areas 2, 4, 6, 7 and 8.